Supplemental Material 1:
Urban Pattern: Layout Design by Hierarchical Domain Splitting

1 Introduction

High-quality layouts of streets and land parcels in a subdivision share several features. Neighboring parcels should have roughly the same size and shape, and to accomodate development of buildings and yards on these parcels, they should be roughly rectangular. Streets should curve smoothly and gently, and meet at roughly right angles. Our paper on street and parcel layout [Anonymous 2013] describes a hierarchical, multiscale approach to subdivision planning that produces designs that satisfy these criteria: at a coarse scale, the subdivision's area is recursively split into smaller regions by placing major streets and thoroughfares along the streamlines of a cross field. At a fine scale, minor streets and individiual land parcels are laid out using a hierarchical template-matching algorithm. This report complements our paper, which focused particularly on the template-based portion of our design framework, by describing in more detail the algorithms we used for generating and selecting the cross fields underpinning the coarse-scale, streamline-based portion of our framework.

As will be discussed below in Section 2, one simple yet powerful approach to laying out streets on a region of land, while maintaining the desired properties of a good layout listed above, is to align the roads along the streamlines of a *cross field* that has *low divergence*. In this report, we present algorithms for generating three different families of such cross fields, each with pros and cons for urban planning:

- **D-fields** based on aligning crosses to the gradient and level sets of the function measuring distance from the subdivision's boundary; and
- **H-fields** generated from the graphs of harmonic functions over the domain; and
- **B-fields** whose iteriors are interpolated smoothly from prescribed boundary orientations.

Sections 4.1, 4.2, and 4.3 discuss these three types of cross fields and their relative advantages.

Although this pipeline can generate high-quality street layouts fully automatically, urban planners often wish to exercise some amount of direction and artistic control over the design. We augment the automatic algorithm to allow a range of such user interactions. Firstly, at each point in layout design, the planners may choose whether the algorithm should generate D-fields, H-fields, or B-fields, and in the case of H-fields, we present the planners with a design gallery of different H-fields from which the most desirable one can be selected. Secondly, as described in our complementary paperm, for all cross field types the user can choose to manually select splitting streamlines or review and possibly veto the automatic suggested selections. Thirdly, the user can select a region of the subdivision and ask that the algorithm recompute and present new options for that region's layout. Lastly, the user has a large amount of control over the template selection and matching process used to lay out fine-level streets and parcels.

2 Modeling Street Layouts as Cross Fields

As mentioned in the introduction, streets in a well-planned network meet at approximately right angles. It is therefore natural to *globally* guide street layout using a *cross field* over the subdivision's domain $\mathcal{R}$. A cross at point $\mathbf{p} \in \mathcal{R}$ is a pair of orthogonal straight lines through $\mathbf{p}$. Each cross can be represented by two unit vectors, leading to four unit vectors $\mathbf{d}^1(\mathbf{p}), \ldots, \mathbf{d}^4(\mathbf{p})$, with consecutive ones forming a right angle. We can uniquely represent the cross as a single unit vector $\mathbf{D}$ (cf. [Palacios and Zhang 2007]): with $\mathbf{d}^i = (\cos u_i, \sin u_i)$, we define $\mathbf{D} := (\cos 4u_i, \sin 4u_i)$, which is obviously independent of the choice of $\mathbf{d}_i,\ i = 1, \ldots, 4$. We call $\mathbf{D}(\mathbf{p})$ the *representation vector field* $\mathcal{V}$ of the cross field $\mathcal{F}$.

A cross field can have *singularities* $\mathbf{s}$, where the cross is undefined. Parallel transport along a closed path around $\mathbf{s}$ yields a non-zero net rotation, and so the cross field cannot be oriented consistently in neighborhoods of such points. By contrast, near a regular point of the cross field, we can find a locally consistent orientation of vector fields $\mathbf{D}$ and $\mathbf{d}^j$. A singularity of a cross field corresponds to a singularity of the vector field $\mathbf{D}$, i.e. $\mathbf{D}(\mathbf{s}) = 0$.

Cross Field Quality and Divergence: Since road placement will be guided by streamlines (integral curves) of the cross field, an ideal cross field has streamlines that are nearly parallel, so that the blocks of land between two roads have approximately the same width. If streamlines are precisely parallel, they form a family of offset curves, and the orthogonal trajectories are straight lines, namely the common normals. This situation is characterized by *vanishing divergence of the unit vector field* $\mathbf{d}^k$ *along the street direction*, which follows immediately from the fact that the curvature of the level sets (here, the normals) of a function equals the divergence of the normalized gradient field (here, $\mathbf{d}^k$). The problem of laying out streets that meet at close to right angles and enclose well-sized parcels of land therefore reduces to the geometry problem of finding cross fields for which one direction $\mathbf{d}^k$ has small divergence.

3 Related Work

The problem of finding such low-divergence cross fields is closely related to that of conformal parameterization and surface quadrangulation, well-studied subjects in geometry processing. Many techniques exist for constructing discrete conformal maps, based on, for instance, least-squares approximation of the Cauchy-Riemann equations [Lévy et al. 2002], minimizing distortion as measured by intrinsic mesh measures [Desbrun et al. 2002], and circle-packings [Kharevych et al. 2006]. Finding a cross field aligned to the boundary is equivalent to finding a conformal map from $\mathcal{R}$ to a planar region with axis-aligned boundaries, but it is unclear how to select such boundaries to minimize cross field divergence.

Early quadrangulation work [Alliez et al. 2003; Marinov and Kobbelt 2004] exploit the observation that principal curvature lines form orthogonal curve networks away from umbilic points, which also forms the basis of the H-fields described below. Other approaches to mesh quadrangulation including using the Morse-Smale complex of the Laplace-Beltrami spectrum to divide the mesh into coarse patches [Dong et al. 2006; Huang et al. 2008]; Palacios and Zhang [2007], Ray et al [2008; 2009] and Bommes et al [2009] work with cross fields directly, interpolating as smoothly as possible user-specified singularities and cross field orientation constraints. These methods seek smooth fields that minimize singularities, but do not address field divergence directly. Such approaches have been used for constructing digital micrograms [Maharik et al. 2011] and for texture synthesis [Xu et al. 2009], and one of our algorithms for frame field design takes advantage of these techniques (see Section 4.3) as well.

4 Cross Field Design

We provide three simple options for generating frame fields for road networks: fields from distance functions *(D-fields)*, from harmonic functions *(H-fields)* optimized for low divergence, and from boundary conditions *(B-fields)*.

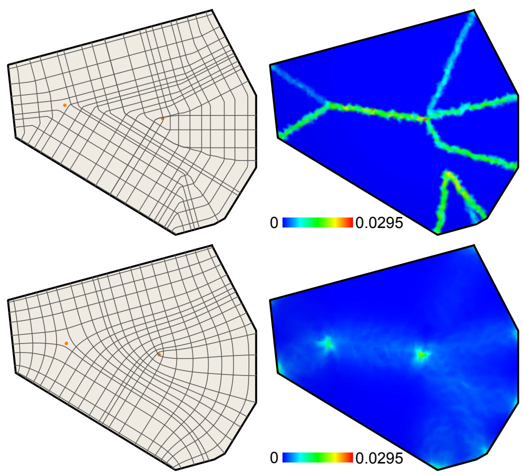

Figure 1: *D-field generation. Top: A weighted distance field defines a cross field which is smooth and exhibits low minimum divergence almost everywhere, except at line features which are at equal weighted distance to two boundary segments; discontinuities are small at those parts of the (weighted) medial axis whose corresponding boundary segments are nearly orthogonal or parallel. Bottom: Smoothing yields aesthetically pleasing flowlines, removes discontinuities and reduces most of the high divergence features.*

4.1 D-Fields: Cross Fields from Distance Functions

Since the cross field should be aligned to tangents and normals of the boundary $\partial\mathcal{R}$ of the given region $\mathcal{R}$, a simple way to obtain a cross field is as follows: For each point $\mathbf{p}$ (not on the medial axis of $\mathcal{R}$), compute the closest boundary point $\mathbf{p}_f$ and define the cross at $\mathbf{p}$ to be parallel and normal to the vector $\mathbf{p}_f - \mathbf{p}$. We call this the *distance cross field of* $\partial\mathcal{R}$. Distance cross fields have discontinuities along the medial axis of $\mathcal{R}$, but many of these can be removed via smoothing. While this works well, it leaves no room for design options and also introduces unnecessary rotation around concave corners.

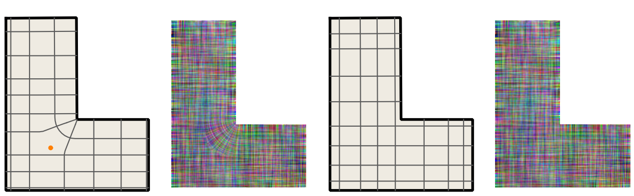

Figure 2: *To avoid unnecessary rotation of crosses around a concave corner in the standard distance function (left), we treat such corners as in a straight skeleton computation (right).*

We now describe a more flexible way of designing good cross fields from distance cross fields (see Fig. 1). The general idea is very simple: We partition $\mathcal{R}$ into regions $\mathcal{R}_k$, define a distance cross field $\mathcal{F}_k$ on each $\mathcal{R}_k$ and apply smoothing to get rid of discontinuities across region boundaries. Since the cross field has to be boundary aligned, we have to involve the distance cross fields of the boundary. Our partitioning into regions $\mathcal{R}_k$ is implicitly provided by a weight function along the boundary of $\mathcal{R}$. For singularity extraction, we use the method of Palacios and Zhang [2007].

We assume that the boundary $\partial\mathcal{R}$ of $\mathcal{R}$ is piecewise smooth. Let $w(\mathbf{r})$ be a weight function which assigns to each boundary point $\mathbf{r} \in \partial\mathcal{R}$ a positive real number. In all our examples, we assign a constant value to each smooth piece of a piecewise smooth boundary; this value determines the influence of the distance field of that piece in the overall design (see Fig. 3). Then, the cross for a point $\mathbf{p} \in \mathcal{R}$ is found as follows:

1. Compute all normal footpoints $\mathbf{p}_f^1, \mathbf{p}_f^2, \ldots \in \partial\mathcal{R}$ of $\mathbf{p}$ (boundary points which are local minima of the distance function to $\mathbf{p}$) and let $\mathbf{p}_f$ be the footpoint with the smallest weighted distance $d^j = \|\mathbf{p} - \mathbf{p}_f^j\| / w(\mathbf{p}_f^j)$ to $\mathbf{p}$.
2. The cross at $\mathbf{p}$ is parallel and normal to the vector $\mathbf{p}_f - \mathbf{p}$; if there is more than one footpoint at closest weighted distance, it is sufficient to take the cross from one of them.
3. The cross field is smoothed as described below.

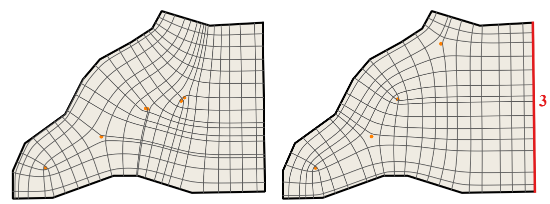

Figure 3: *By default, we use weight* 1 *for all boundary segments (left). Increasing the weight of a segment enlarges the influence of its distance field on the final D-field (right).*

Concave Corners: If a footpoint $\mathbf{p}_f^k$ is a corner (hence, concave), we do not take the distance to the corner (to avoid rotation, see Fig. 2), but use distances to the two tangents T_1, T_2 at $\mathbf{p}_f^k$ like in the case of a (weighted) straight skeleton. We compute the weighted signed distances to T_1, T_2 and define d^k to be the larger of these values. The cross is parallel and normal to the corresponding tangent.

Smoothing: In practice, we triangulate the input region [Shewchuk 1996] with Steiner points and compute the cross field over the vertices of the underlying triangulated mesh M. This field contains singularities along the domain's medial axes; to improve the quality of the field's streamlines, we apply one round of smoothing after generating the cross field. The representation vector $\mathbf{D}_i$ at each interior vertex i is averaged with the vectors at its incident neighbors, followed by renormalization of the vectors.

4.2 H-Fields: Cross Fields from Harmonic Functions

We have implemented another way for generating a cross field, which may have larger divergence, but has the great advantage of providing more design inspiration in very simple cases. While the D-fields will always recover the trivial Cartesian grid if the boundary is taken from it, the method described below comes up with more creative design variants (see Fig. 4).

This second approach to generating a frame field on $\mathcal{R}$ is based on graphs of harmonic functions $z(\mathbf{p})$, $\Delta z = 0$ over $\mathcal{R}$. Such surfaces are the analogue to minimal surfaces in *isotropic geometry.* In

Euclidean geometry, minimal surfaces are isothermic – their principal curvature lines follow a conformal parameterization of that surface. Similarly, graphs of harmonic functions are isotropic isothermic surfaces; the isotropic principal curvature directions, given by eigenvectors of the Hessian Hz conformally parameterize $\mathcal{R}$. Laying out roads along such a cross field therefore yields parcels that are particularly well-proportioned.

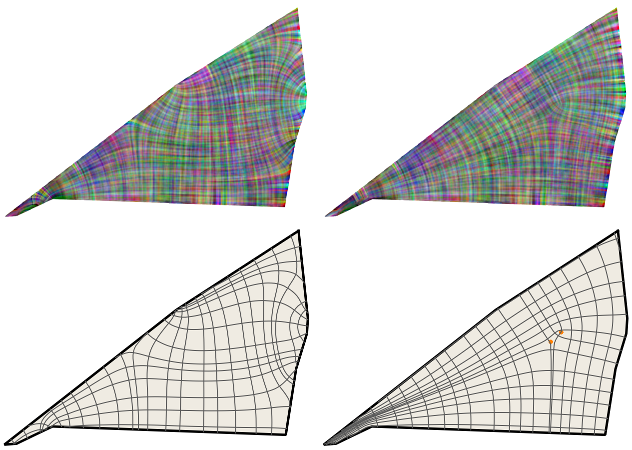

Figure 4: *H-fields (left) tend to provide more creative design options, while D-fields (right) usually have lower divergence and less singularities close to the boundary.*

We need the cross field to be adapted to the boundary of $\mathcal{R}$: it must satisfy $(\mathbf{d}^1 \cdot \mathbf{n})(\mathbf{d}^2 \cdot \mathbf{n}) = 0$ on $\partial\mathcal{R}$, where $\mathbf{n}$ is the outward-pointing boundary normal. If Hz has distinct eigenvalues, this condition is equivalent to

$$\mathbf{n}^T HzJ\mathbf{n} = 0 \tag{1}$$

on $\partial\mathcal{R}$, where $J = \begin{bmatrix} 0 & -1 \\ 1 & 0 \end{bmatrix}$ is rotation by 90 degrees.

Condition (1) is particularly simple if the boundary of $\mathcal{R}$ is piecewise linear. Let $\gamma_i(s)$ be an arc-length parameterization of a piece r_i of the boundary, so that $\mathbf{n} = J\widehat{\gamma_i'}$ is constant and $\mathbf{n}' = 0$. Then

$$\begin{aligned} \frac{d}{ds}(\nabla z \cdot \mathbf{n}) &= \gamma_i'^T Hz\,\mathbf{n} + \nabla z \cdot \mathbf{n}' \\ &= \mathbf{n}^T Hz\,\gamma_i' = \frac{1}{\|\gamma_i'\|}\mathbf{n}^T Hz\,J\mathbf{n} = 0. \end{aligned}$$

Thus the harmonic functions z whose Hessians have eigenvectors parallel and tangent to the boundary are precisely those satisfying

$$\begin{cases} \Delta z(\mathbf{p}) = 0, & \mathbf{p} \in \mathcal{R} \\ \nabla z \cdot \mathbf{n} = c_i, & \mathbf{p} \in r_i \end{cases} \tag{2}$$

for constants c_i. This boundary value problem has a unique solution whenever the c_i obey the compatibility conditions imposed by Gauss's theorem:

$$0 = -\int_{\mathcal{R}} \Delta z\, dA = \int_{\partial\mathcal{R}} \nabla z \cdot \mathbf{n}\, dS = \sum_i \int_{r_i} c_i = \sum_i \ell_i c_i,$$

where ℓ_i is the length of the boundary segment r_i.

Discretization: For any choice of c_i, the corresponding adapted frame field $\mathbf{D}$ can be approximated by solving the discretization $Lz = b$ of the Poisson problem with Neumann boundary conditions (2) (where L is the well-known "cotan weight" discrete Laplace-Beltrami operator [Pinkall and Polthier 1993]), approximating the Hessian of z using quadric fitting, calculating the eigenvectors $\mathbf{d}^k$, and extending this tensor field to the interior of triangles by linear interpolation. This tensor field can be converted to a cross field locally (for blending or following flow lines) by consistently orienting the principle eigenvector.

Finding Boundary Conditions through Optimization: We seek cross fields with low divergence along at least one direction $\mathbf{d}^k$. The above procedure for generating frame fields from harmonic functions has $k-1$ degrees of freedom c_i, where k is the number of boundary segments; there is thus room to search for low-divergence cross fields through optimization.

Consider the following cross field energy:

$$E(\mathbf{D}) = \int_{\mathcal{R}} \left(\nabla \cdot \mathbf{d}^1\right)^2 dA.$$

From an initial choice of c_i, this energy is used to relax the cross field to one with less divergence. We use gradient descent to find a local minimum, estimating the gradient search direction δc_i by numerically differentiating E with finite differences. The size of the step is calculated using a line search; the directional derivative of E along δc_i is given by

$$\begin{aligned} &\left[\frac{d}{dt}\int_{\mathcal{R}} \left(\nabla \cdot \frac{\mathbf{d}^1 + t\delta\mathbf{d}^1}{\|\mathbf{d}^1 + t\delta\mathbf{d}^1\|}\right)^2 dA\right]\Bigg|_{t=0} \\ &= \int_{\mathcal{R}} \left(\nabla \cdot \frac{\mathbf{d}^1}{\|\mathbf{d}^1\|}\right) \nabla \cdot \left(\frac{\delta\mathbf{d}^1}{\|\mathbf{d}^1\|} - \frac{\mathbf{d}^1(\mathbf{d}^1 \cdot \delta\mathbf{d}^1)}{\|\mathbf{d}^1\|^3}\right) dA. \end{aligned}$$

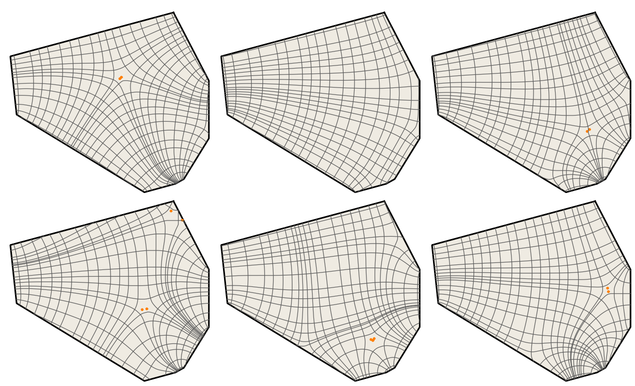

Figure 5: *The degrees of freedom in H-fields can be used to present the user with a design gallery (local minima of an optimization for low divergence).*

Since E is nonconvex, and since an optimal street layout involves aesthetic criteria beyond low divergence, we allow the user to choose from several local minima presented in a gallery (Fig. 5). A less symmetric alternative to defining the cross field by the eigenvectors of Hz would be to let the crosses be parallel and orthogonal to the gradient ∇z of a harmonic function z (see [Dong et al. 2005]). However, the space of such cross fields is less easy to parameterize and explore, since one has two options at each smooth piece of the boundary: whether ∇z is normal or tangent to it.

4.3 B-Fields: Interpolation from the Boundary

The last option presented to the user for cross field design constructs the field by fitting a smooth cross field to the boundary, along the lines of the algorithm used by Maharik et al [2011]. Unlike D- or

H-fields, B-fields are not explicitly constructed to minimize divergence (a disadvantage most obvious on irregularly-shaped domains such as the one in Fig. 6, right), but on the other hand B-field streamlines typically adhere well to the global shape of the domain and have few singularities, and thus are a valuable design option for planning street layout.

At each vertex i on the boundary, an initial cross field vector $\tilde{\mathbf{d}}_i^1$ is computed by averaging the incident oriented boundary edge vectors. From these vectors, we calculate the initial representation vector $\tilde{\mathbf{D}}_i$ on that vertex, as described in Section 2. Notice that this representation vector encodes that the cross field should be aligned to the boundary, but does not specify a precise cross orientation.

From this initial boundary data, we construct the full representation vector field $\mathbf{D}$ by solving the quadratic variational problem

$$\min_{\mathbf{D}} \sum_{i,j} \|\mathbf{D}_i - \mathbf{D}_j\|^2 + \omega \sum_{i \in \text{bdry}} \|\mathbf{D}_i - \tilde{\mathbf{D}}_i\|^2,$$

where the first sum is over all pairs of incident vertices i, j and the second sum is over the boundary vertices. The user-specified weight ω trades off between keeping the cross field adapted to the boundary, and increasing field smoothness (see Fig. 6). The new representation vectors $\mathbf{D}_i$ are not necessarily unit length, and are thus renormalized.

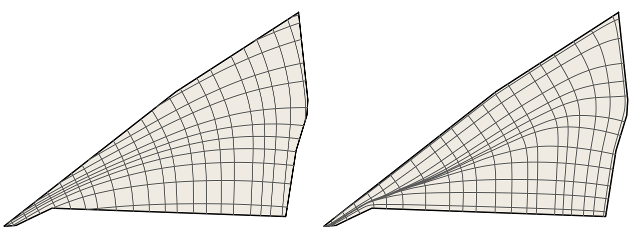

Figure 6: *B-fields with $\omega = 0.1$ (left) and $\omega = 0.9$ (right). Decreasing the weight increases the cross field smoothness, at the cost of decreasing alignment of the cross field with the boundary.*

5 Conclusion

Since streets in high-quality subdivision layouts are nearly parallel, and meet at roughly right angles, our urban planning algorithm lays out major roads along streamlines of *low-divergence cross fields*. This model transforms the problem of finding road layouts satisfying these design goals into a computational geometry problem. We described three algorithms for generating such cross fields, based on the distance function to the boundary (D-fields), graphs of harmonic functions (H-fields), and solving for smooth fields interpolating the boundary (B-fields). The next steps in the urban planning pipeline, from placing roads by hierarchically selecting high-quality cross field streamlines, to the design of minor streets and land parcels using template warping, is discussed in detail in the accompanying paper [Anonymous 2013].

We allow user intervention at all stages of the planning process; at the cross field design stage, the user may set boundary influence weights (for D-fields), choose from among several candidate cross fields in a design gallery (for H-fields), and control smoothness versus boundary alignment (for B-fields). Several interesting avenues of future work could extend the user's influence over this step of design: some ideas include allowing manual placement of singularities (intersections, roundabouts) and incorporating sketched suggestions of where roads should be placed. It would also be interesting to augment our algorithms to make use of three-dimensional topographic information about the land, which would allow planning of roads that follow geographic features, minimize elevation changes, etc.

References

ALLIEZ, P., COHEN-STEINER, D., DEVILLERS, O., LÉVY, B., AND DESBRUN, M. 2003. Anisotropic polygonal remeshing. *ACM Trans. on Graph. 22*, 3.

ANONYMOUS. 2013. Urban pattern: Layout design by hierarchical domain splitting. *In Preparation*.

BOMMES, D., ZIMMER, H., AND KOBBELT, L. 2009. Mixed-integer quadrangulation. *ACM Trans. on Graph. 28*, 3.

DESBRUN, M., MEYER, M., AND ALLIEZ, P. 2002. Intrinsic parameterizations of surface meshes. *Computer Graphics Forum 21*, 3.

DONG, S., KIRCHER, S., AND GARLAND, M. 2005. Harmonic functions for quadrilateral remeshing of arbitrary manifolds. *Computer Aided Geometric Design 22*, 5, 392–423.

DONG, S., BREMER, P.-T., GARLAND, M., PASCUCCI, V., AND HART, J. 2006. Spectral surface quadrangulation. *ACM Trans. on Graph. 25*, 3.

HUANG, J., ZHANG, M., MA, J., LIU, X., KOBBELT, L., AND BAO, H. 2008. Spectral quadrangulation with orientation and alignment control. *ACM Trans. on Graph. 27*, 5.

KHAREVYCH, L., SPRINGBORN, B., AND SCHRÖDER, P. 2006. Discrete conformal mappings via circle patterns. *ACM Trans. on Graph. 25*, 2.

LÉVY, B., PETITJEAN, S., RAY, N., AND MAILLOT, J. 2002. Least squares conformal maps for automatic texture atlas generation. *ACM Trans. on Graph. 21*, 3, 362–371.

MAHARIK, R., BESSMELTSEV, M., SHEFFER, A., SHAMIR, A., AND CARR, N. 2011. Digital micrography. *Transactions on Graphics (Proc. SIGGRAPH 2011)*, 100:1–100:12.

MARINOV, M., AND KOBBELT, L. 2004. Direct anisotropic quad-dominant remeshing. In *Proceedings of the Computer Graphics and Applications, 12th Pacific Conference*.

PALACIOS, J., AND ZHANG, E. 2007. Rotational symmetry field design on surfaces. *ACM Trans. on Graph. 26*, 3.

PINKALL, U., AND POLTHIER, K. 1993. Computing discrete minimal surfaces and their conjugates. *Experimental Mathematics 2*, 15–36.

RAY, N., VALLET, B., LI, W. C., AND LÉVY, B. 2008. N-symmetry direction field design. *ACM Trans. on Graph. 27*, 2.

RAY, N., VALLET, B., ALONSO, L., AND LVY, B. 2009. Geometry-aware direction field processing. *ACM Trans. on Graph. 29*, 1.

SHEWCHUK, J. R. 1996. Triangle: Engineering a 2D Quality Mesh Generator and Delaunay Triangulator. In *Applied Computational Geometry: Towards Geometric Engineering*, Springer-Verlag, M. C. Lin and D. Manocha, Eds., vol. 1148, 203–222.

XU, K., COHEN-OR, D., JU, T., LIU, L., ZHANG, H., ZHOU, S., AND XIONG, Y. 2009. Feature-aligned shape texturing. *ACM Transactions on Graphics, (Proceedings SIGGRAPH Asia 2009) 28*, 5, 108:1–108:7.